Available online at www.sciencedirect.com
ScienceDirect
Physica E 40 (2008) 920–923
PHYSICA E
www.elsevier.com/locate/physe

Photoluminescence and Raman analysis of ZnO nanowires deposited on Si(1 0 0) via vapor–liquid–solid process

Li-li Yang[a,b,c], Jing-hai Yang[a,c,*], Dan-dan Wang[a,b,c], Yong-jun Zhang[a], Ya-xin Wang[a], Hui-lian Liu[a], Hou-gang Fan[a], Ji-hui Lang[a]

[a]*Key Laboratory of Excited State Processes, Changchun Institute of Optics, Fine Mechanics and Physics, Chinese Academy of Sciences, Changchun 130033, People's Republic of China*
[b]*Graduate School of the Chinese Academy of Sciences, Beijing 100049, People's Republic of China*
[c]*Institute of Condensed State Physics, Jilin Normal University, Siping 136000, People's Republic of China*

Received 24 April 2007; received in revised form 24 September 2007; accepted 15 November 2007
Available online 11 January 2008

Abstract

ZnO nanowires were deposited on the Si(1 0 0) substrate via vapor–liquid–solid process with flowing Ar gas current for 90 s. The morphology, structure, and optical properties were investigated by scanning electron microscopy (SEM), X-ray diffraction (XRD), photoluminescence (PL), and Raman spectrum, respectively. The results showed that the as-deposited ZnO nanowires had hexagonal wurzite structure. The Raman spectrum showed oxygen defects in ZnO nanowires due to the existence of the Ar gas during the growth process, leading to the dominant green band peak and the weak UV peak in the PL spectrum. And blue shift of the Raman peaks was attributed to the lattice distortion and piezoelectric effect of the nanostructures. Finally, the biaxial compressive stress within the *c*-axis oriented ZnO nanowires was estimated to 0.365 GPa, which was also responsible for the frequency shift of the E_2 (high) mode of the Raman spectra.

PACS: 61.82.Fk; 74.25.Gz; 81.10.−h

Keywords: ZnO nanowires; Photoluminescence; Raman; Vapor–liquid–solid process

1. Introduction

In recent years, one-dimensional (1D) nanostructures such as nanotubes [1], nanowires [2], nanorods [3], nanobelts [4], nanocables [5], and nanoribbons [6] stimulate considerable interests for scientific research due to their importance in fundamental physics studies and their potential applications in nanoelectronics, nanomechanics, and flat-panel displays. Among various 1D nanostructural materials, zinc oxide generates great interests for its direct wide band gap of 3.37 eV, large exciton binding energy of 60 meV, and stable physical and chemical properties. One of the representative 1D ZnO nanostructures is nanowires. So far, many efforts are made for achieving ZnO nanowires, including physical evaporation [7], chemical vapor deposition [8–10], and solvothermal method [11,12] on different substrates. High-quality ZnO nanowires and thin film are mainly deposited on sapphire substrates [13–15]. Nevertheless, sapphire is not conductive and rather expensive, which may pose a serious limitation on the applications of the nanowire arrays in optoelectronic devices. In the pursuit of the next-generation semiconductor nanowire-based optoelectronic nanodevices, it would be highly desirable well-ordered nanowires be directly aligned on a conductive and low-cost substrate, such as the Si wafer. Unfortunately, the large mismatches in the thermal expansion coefficients and the lattice constants would introduce rather large stress between the ZnO and the Si wafer. Previous efforts in preparing the well-oriented ZnO nanowire arrays on the Si wafer have not reached satisfactory quality [16]. Therefore, more research on the

*Corresponding author. Tel.: +86 434 3290009; fax: +86 434 3294566.
E-mail address: jhyang1@jlnu.edu.cn (J.-h. Yang).

1386-9477/$ - see front matter © 2007 Elsevier B.V. All rights reserved.
doi:10.1016/j.physe.2007.11.025

preparing conditions with different methods should be done in the following days.

In this investigation, scanning electron microscopy (SEM), X-ray diffraction (XRD), photoluminescence (PL), and Raman scattering were performed to characterize the as-deposited ZnO nanowires arrays on Si(1 0 0) substrate by the vapor–liquid–solid (VLS) technique and the magnitude of the stress between the ZnO nanowires and Si substrate was also estimated from the Raman spectra.

2. Experimental

Synthesis of the ZnO nanowire arrays was carried out in a conventional furnace with a horizontal quartz tube. In a typical process, an Au layer of 2 nm in thickness was first thermally evaporated onto the polished side of a Si(1 0 0) substrate to serve as catalyst. The Au-coated side faced downward on an alumina boat loaded with the mixture powder of ZnO (99.99%, 325 mesh, Alfa Aesar) and carbon (99.99%, 325 mesh, Alfa Aesar) with 1:1 ratio. And then, the alumina boat was transferred into the center of a small quartz tube avoiding the pollution. At last, the small quartz tube was placed inside a horizontal tube furnace. The initial temperature of the furnace was 850 °C. The temperature of the furnace was synchronously ramped to 900 °C rapidly with Ar gas flowing for the first 90 s. Then, the furnace was kept at the temperature of 900 °C for 1 h. After cooling down, light or dark gray film was found over the Au-coated Si(1 0 0) substrates. The supply current of Ar gas is 3 L min^{-1}. When the supply time of Ar gas is shorter or longer then 90 s, ZnO nanowires cannot be obtained as reported in our previous works [17].

The as-synthesized products were characterized by XRD (MAC Science, MXP18, Japan) and SEM (Hitachi, S-570). PL measurements were carried out at room temperature. A He–Cd laser with 325 nm emission was used for PL excitation. Raman spectra were measured with a Jobin Yvon LABRAM-UV Raman spectrometer. The accuracy of Raman spectrum is better than 0.4 cm^{-1}. A He–Ne laser with 633 nm emission line was used as the excitation source.

3. Results and discussions

Fig. 1 shows the typical morphology with different magnification of the ZnO sample deposited on Si(1 0 0) substrate. The ZnO nanowires of high density showed grass-like morphology and the angle between nanowires and substrate plane was in the range of 45–80°. The diameter of these ZnO nanowires varied from 50 to 300 nm, with an average around 180 nm. The average ratio of length/diameter of the ZnO nanowires was estimated larger than 13. The magnified view of a single nanowire showed the hexagonal facets of the nanowire tip.

The XRD spectrum shown in Fig. 2 agreed with the standard card of bulk ZnO with hexagonal structure (JCPDS No. 800075) and no diffraction peaks of other impurities were detected. Moreover, the strong intensity and narrow width of ZnO diffraction peaks also indicated that the resulting product was of better crystallinity. The (0 0 2) peak at 34.4° was dominant, indicating that ZnO sample was oriented and the growth direction was along (0 0 1). The peaks (1 0 0), (1 0 1), (1 0 2), and (1 1 0) indicated that the nonepitaxial growth took place. The XRD analysis

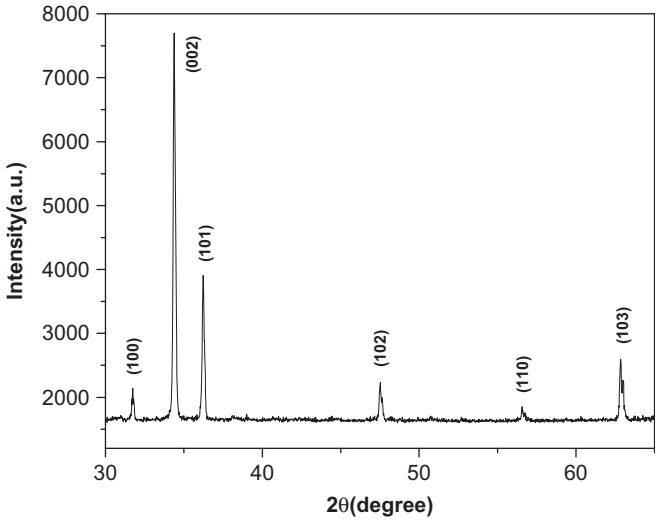

Fig. 2. XRD patterns of ZnO nanowires deposited on Si(1 0 0) substrate.

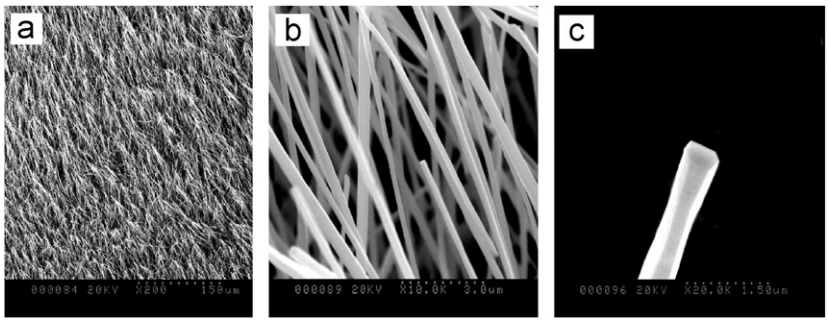

Fig. 1. SEM images of ZnO nanowires deposited on Si(1 0 0) substrate.

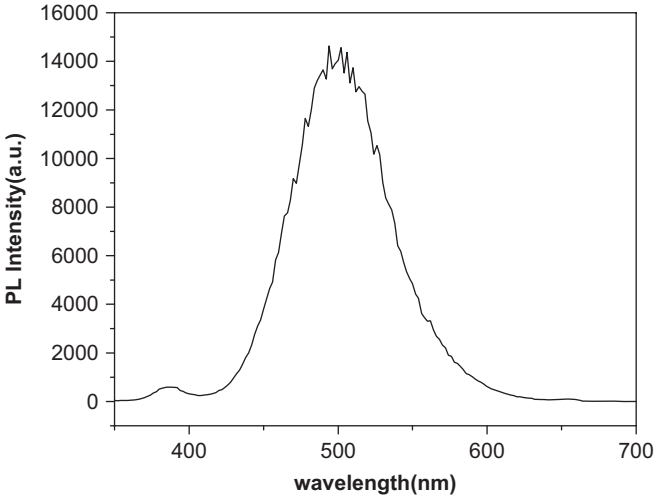

Fig. 3. PL spectrum of ZnO nanowires grown on Si(1 0 0) substrate.

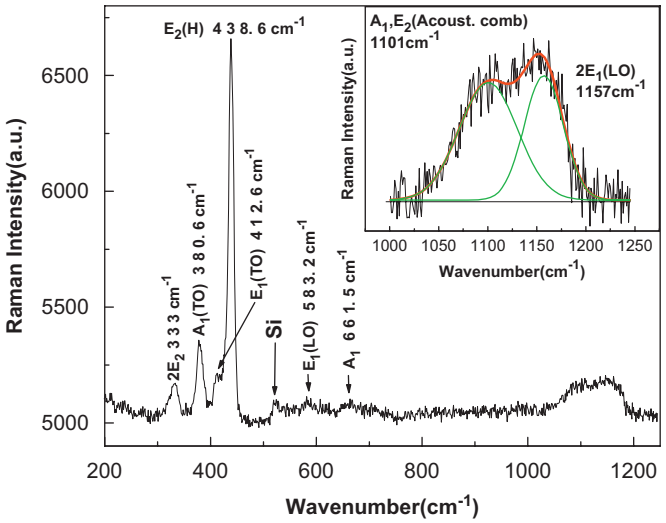

Fig. 4. Raman spectrum of ZnO nanowires grown on Si(1 0 0) substrate.

results were in good agreement with the SEM images shown in Fig. 1.

Fig. 3 shows the PL spectrum measured at room temperature consisting of a weak UV peak at 385 nm in wavelength and a dominant green band with a broad feature in the range of 420–600 nm. The UV emission band was related to a near band-edge transition of ZnO, namely, the recombination of free excitons through an exciton–exciton collision process [18]. The green band was generally explained by the radial recombination of a photogenerated hole with the electron in a singly ionized oxygen vacancy [19]. The weak UV emission and the strong green band in the PL spectra indicated that the as-synthesized ZnO nanowires had more oxygen vacancies. This could be explained by the growth mechanism of VLS technique with the involvement of Ar gas. The growth process could be expressed as following [20,21]:

$$ZnO_{(s)} + C_{(s)} \rightarrow Zn_{(g)} + CO_{(g)}, \quad (1)$$

$$CO_{(g)} + ZnO_{(s)} \rightarrow CO_{2(g)} + Zn_{(g)}, \quad (2)$$

$$Zn_{(g)} + CO_{(g)} \rightarrow ZnO_{(s)} + C_{(s)}, \quad (3)$$

$$2Zn_{(g)} + O_{2(g)} \rightarrow 2ZnO_{(s)}, \quad (4)$$

$$C_{(g)} + CO_{2(g)} \rightarrow 2CO_{(g)}. \quad (5)$$

According to Eqs. (3) and (4), O_2 and CO provided the oxygen source of the ZnO nanowires. In our experiments, the main difference from the common VLS method was that the substrates were on top of the powder and there was no need for a carrier gas. Therefore, Ar gas did not act as transportation gas but only adjusted the ambient gas composition in the furnace, especially the O concentration. Once the Ar gas current flew into the furnace, the O concentration decreased, and then more oxygen vacancies formed in ZnO nanowires, which made the green band enhanced and even became the dominant peak in the PL spectrum.

The space group of the hexagonal wurzite ZnO belongs to C_{6v}^4, with two formula units per primitive cell. According to the group theory, single-crystalline ZnO has eight sets of optical phonon modes at Γ point of the Brillouin zone, classified as $A_1 + E_1 + 2E_2$ modes (Raman active), $2B_1$ modes (Raman silent), and $A_1 + E_1$ modes (infrared active). Moreover, the A_1 and E_1 modes split into LO and TO components. Fig. 4 shows the Raman spectrum of ZnO nanowires deposited on Si(0 0 1) substrate, where the peaks at 332.3, 380.6, 438.6, 583.2, and 661.5 cm^{-1} were clearly observed in the low wave-number region. Moreover, there was a very weak shoulder located at the low energy side of 438.6 cm^{-1} peak, which corresponded to the E_1(TO) at 412.6 cm^{-1}. On the other hand, a broad asymmetrical peak located at the large wave-number region from 1000 to 1300 cm^{-1}. It was fitted with Gaussian functions, where Gaussian functions gave clearly better disconsolations. Two Gaussian curves were extracted for the spectrum (see the inset), and two peaks located at 1101 and 1157 cm^{-1}, respectively. No more high-order peaks could be observed in the region over 1300 cm^{-1}. All peaks were assigned on the basis of group theoretical analysis. The results as well as a comparison with the previous work of bulk crystal are listed in Table 1.

The E_2(high), A_1(TO), E_1(TO), and E_1(LO) mode showed 1.6, 0.6, 5.6, and 0.2 cm^{-1} blue shift, respectively, compared with bulk material [22]. Two reasons may be responsible for the blue shift. One is the lattice distortion caused by the oxygen vacancies. Another reason is that the nanostructures possess piezoelectric effect, which causes the shift of Raman modes, as the confinement is anisotropic which has different effect on different phonon modes, and as a result the blue shift of each mode is different.

E_2(high) is usually used to analyze the stress state in films due to its high sensitivity to stress [23]. So, the frequency

Table 1
Wave number (in cm^{-1}) and symmetries of the modes found in Raman spectrum of hexagonal ZnO nanowires and their assignments

Wave number	Symmetry	Process	Ref. [22] (bulk crystal)
332.3	A_1	Acoustic overtone	
380.6	A_1(TO)	First process	380
412.6	E_1(TO)	First process	407
438.6	E_2(High)	First process	437
583.2	E_1(LO)	First process	583
661.5	A_1	Acoustic overtone	
1101	A_1, E_2	Acoustic combination	
1157	A_1	Optic overtone	

shift of the E_2(high) mode is also attributed to the stress variation. Decremps et al. pointed out that the E_2 mode of the wurzite ZnO crystal would shift to a higher frequency under the biaxial compressive stress within the *c*-axis oriented ZnO epilayers by $\Delta\omega\ (cm^{-1}) = 4.4\sigma$ (GPa) [24]. It was been used to estimate the magnitude of the stress between the ZnO nanowires and the Si substrate from the Raman spectra. In our case, the frequency of the E_2 mode observed in the as-synthesized ZnO nanowires arrays was $1.6\,cm^{-1}$ higher than that observed in the bulk ZnO crystal [22]. The blue shift of the E_2 mode corresponding to the $437\,cm^{-1}$ of the bulk crystal demonstrated that the ZnO nanowires grown on the Si substrate are under compressive stress, which was estimated to be 0.365 GPa. It was reported that the biaxial compressive stress within the ZnO films on Si(1 0 0) was in the range of 0.9–9.9 GPa [25]. The smaller stress of the ZnO nanowires arrays compared with that of the ZnO films should be attributed to the stress relaxation effect from the ZnO nanowires. However, it was reported that the biaxial compressive stress within the ZnO nanowires Si(1 0 0) was 0.225 GPa estimated with the same model [26]. The larger stress of our sample could be attributed to the more oxygen defects in the ZnO nanowires, which made the lattice distorted.

In addition, the existence of the E_1(LO) mode indicated more defects, because E_1(LO) was associated with lattice defects, such as oxygen vacancy and zinc interstitial [27], which testified the results of the PL spectrum further.

4. Conclusion

In summary, ZnO nanowires with hexagonal wurzite structure were successfully fabricated on the Si(1 0 0) substrate via vapor–liquid–solid process with flowing Ar gas current for 90 s. SEM results showed that the angle between nanowires and substrate plane is in the range of 45–80°. The average diameter and ratio of length/diameter of the ZnO nanowires was around 180 nm and larger than 13, respectively. PL and Raman results showed that Ar was not beneficial to the growth of ZnO nanowires via the VLS technique because there were more oxygen vacancies in our nanowires.

Acknowledgments

We would like to thank the financial support of National Nature Science Foundation of China (NNSFC, No. 60778040), Science and Technology Bureau of Jilin Province (No. 20060518), Education Bureau of Jilin Provice(No. 2007363,2007162,2007149) and Gifted Youth Program of Jilin Province (No. 20060123, 20070118).

References

[1] S. Iijima, Nature 354 (1991) 56.
[2] M.H. Huang, S. Mao, H. Feick, et al., Science 292 (2001) 1897.
[3] J.Y. Li, X.L. Chen, H. Li, et al., J. Cryst. Growth 233 (2001) 5.
[4] Z.W. Pan, Z.R. Dai, Z.L. Wang, Science 291 (2001) 1947.
[5] J. Wu, S. Liu, C. Wu, et al., Appl. Phys. Lett. 81 (2002) 1312.
[6] B.D. Yao, Y.F. Chan, N. Wang, Appl. Phys. Lett. 81 (2002) 757.
[7] S.C. Lyu, Y. Zhang, C.J. Lee, Chem. Mater. 15 (2003) 3294.
[8] Y.K. Tseng, C.J. Huang, H.M. Cheng, et al., Adv. Funct. Mater. 13 (2003) 811.
[9] C.J. Lee, T.J. Lee, S.C. Lyu, et al., Appl. Phys. Lett. 81 (2002) 3648.
[10] J. Park, H.-H. Choi, K. Siebein, et al., J. Cryst. Growth 258 (2003) 342.
[11] L. Vayssieres, Adv. Mater. 15 (2003) 464.
[12] L.E. Greene, M. Law, J. Goldberger, et al., Angew. Chem. 115 (2003) 3139.
[13] H. Cao, J.Y. Xu, D.Z. Zhang, et al., Phys. Rev. Lett. 84 (2000) 5584.
[14] W.I. Park, D.H. Kim, S.W. Jung, G.-C. Yi, Appl. Phys. Lett. 80 (2002) 4232.
[15] H. Kim, W. Sigmund, Appl. Phys. Lett. 81 (2002) 2085.
[16] Y. Zhang, H. Jia, R. Wang, et al., Appl. Phys. Lett. 83 (2005) 4631.
[17] J. Yang, D. Wang, L. Yang, et al., J. Alloys Compd., 〈doi:10.1016/j.jallcom.2006.11.160〉.
[18] Y.C. Kong, D.P. Yu, B. Zhang, et al., Appl. Phys. Lett. 78 (2001) 407.
[19] K. Vanheusden, W.L. Warren, C.H. Seager, et al., J. Appl. Phys. 79 (1996) 7983.
[20] J. Wang, J. Sha, Q. Yang, et al., Mater. Lett. 59 (2005) 2710.
[21] M.H. Huang, Y. Wu, et al., Adv. Mater. 13 (2001) 113.
[22] T.C. Damen, S.P.S. Porto, B. Tell, Phys. Rev. 142 (2001) 570.
[23] S. Tripathy, S.J. Chua, P. Chen, Z.L. Miao, J. Appl. Phys. 92 (2002) 3503.
[24] F. Decremps, J.P. Porres, A.M. Saitta, et al., Phys. Rev. B 65 (2002) 092101.
[25] S.W. Whangbo, H.K. Jang, S.G. Kim, et al., J. Korean Phys. Soc. 37 (2000) 456.
[26] Y. Zhang, H. Jia, R. Wang, Appl. Phys. Lett. 83 (2003) 4631.
[27] X. Wang, Q. Li, Z. Liu, J. Zhang, et al., Appl. Phys. Lett. 84 (2004) 4941.